Author/s:
Yaghoubzadehfard, A;Zhou, Z;Herath, N;Sofi, M;Lumantarna, E;Mendis, P;Vaz-Serra, P;Day, K;Ma, X

Title:
Structural evaluation of a 1971 reinforced concrete building with limited documentation: a hybrid experimental-numerical approach

Date:
2026

Citation:
Yaghoubzadehfard, A., Zhou, Z., Herath, N., Sofi, M., Lumantarna, E., Mendis, P., Vaz-Serra, P., Day, K. & Ma, X. (2026). Structural evaluation of a 1971 reinforced concrete building with limited documentation: a hybrid experimental-numerical approach. Australian Journal of Structural Engineering, 27 (1), pp.1-14. https://doi.org/10.1080/13287982.2026.2625342.

Persistent Link:
https://hdl.handle.net/11343/366914

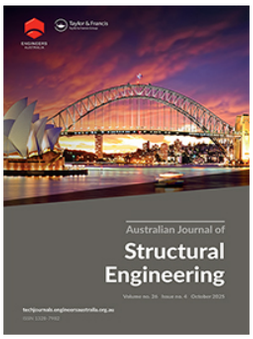

Australian Journal of Structural Engineering

ISSN: 1328-7982 (Print) 2204-2261 (Online) Journal homepage: www.tandfonline.com/journals/tsen20

# Structural evaluation of a 1971 reinforced concrete building with limited documentation: a hybrid experimental-numerical approach

A. Yaghoubzadehfard, Z. Zhou , N. Herath , M. Sofi , E. Lumantarna , P. Mendis , P. Vaz-Serra , K. Day & X. Ma

**To cite this article:** A. Yaghoubzadehfard, Z. Zhou , N. Herath , M. Sofi , E. Lumantarna , P. Mendis , P. Vaz-Serra , K. Day & X. Ma (04 Feb 2026): Structural evaluation of a 1971 reinforced concrete building with limited documentation: a hybrid experimental-numerical approach, Australian Journal of Structural Engineering, DOI: 10.1080/13287982.2026.2625342

**To link to this article:** https://doi.org/10.1080/13287982.2026.2625342



Published online: 04 Feb 2026.

AUSTRALIAN JOURNAL OF STRUCTURAL ENGINEERING
https://doi.org/10.1080/13287982.2026.2625342

Taylor & Francis
Taylor & Francis Group



# Structural evaluation of a 1971 reinforced concrete building with limited documentation: a hybrid experimental-numerical approach

A. Yaghoubzadehfard [a], Z. Zhou[a], N. Herath[a], M. Sofi[a], E. Lumantarna[a], P. Mendis[a], P. Vaz-Serra[b], K. Day[b] and X. Ma[b]

[a]Department of Infrastructure Engineering, The University of Melbourne, Parkville, VIC, Australia; [b]Faculty of Architecture Building and Planning School of Design, The University of Melbourne, Parkville, VIC, Australia

**ABSTRACT**

This study proposes a comprehensive methodology for the structural health assessment of ageing infrastructure with limited available documentation. The case study involves a reinforced concrete structure constructed in 1971, for which only architectural drawings with a limited technical document are available. An initial finite element model (FEM) is developed based on geometric information inferred from the available drawings and standard material assumptions. To overcome uncertainties arising from the absence of structural and reinforcement details, a suite of non-destructive tests, Schmidt hammer rebound tests and Profometer are employed. The experimental results are used to update and calibrate the FEM, enabling a more accurate representation of the in-situ condition. The refined model is then used to evaluate structural performance and compare results against current design codes. This integrated approach highlights the value of combining limited documents with in-situ testing to support informed decision-making in the assessment and management of ageing concrete. When reassessed against AS 1170 and AS 3600 provisions, the structure failed to meet key performance requirements, particularly in lateral resistance and reinforcement capacity, highlighting the need for retrofit.

**ARTICLE HISTORY**
Received 1 October 2025
Accepted 26 January 2026

**KEYWORDS**
Structural health assessment; finite element model; aged RC buildings; code compliance; limited documents

## 1. Introduction

A large proportion of reinforced concrete (RC) infrastructure currently in service was constructed several decades ago, often without the benefit of detailed documentation or consistent material records. As these structures age, concerns regarding their ongoing safety, serviceability, and compliance with modern standards continue to grow. Timely structural assessment is therefore essential to support maintenance planning, risk mitigation, and asset management decisions. However, the evaluation of aged structures is often complicated by missing or incomplete construction records, particularly the absence of structural or reinforcement drawings, which presents a significant challenge to engineers and asset owners.

In such cases, traditional assessment approaches that rely heavily on comprehensive design documentation become inadequate. This has driven the development of hybrid strategies that integrate limited archival information with in-situ measurements obtained through non-destructive testing (NDT). NDT techniques (e.g. Ground Penetrating Radar, Schmidt hammer testing, Profometer etc.) enable valuable insights into reinforcement layout, surface hardness, and durability without intrusive intervention. When paired with finite element modelling (FEM), these techniques provide a pathway to reconstruct the structural condition and assess performance under contemporary loading and code requirements.

The accurate assessment of in-situ concrete strength remains a priority for civil engineers, particularly when evaluating ageing reinforced concrete structures. Traditional methods, such as core sampling, while precise, are often destructive, time-consuming, and impractical for widespread use. Therefore, NDT methods such as the Schmidt Hammer have gained significant attention for offering rapid, low-cost, and in-place evaluation of surface hardness and strength characteristics (Alyamac, Ghafari, and Ince 2017; Yılmaz & Avşar 2013; Yon et al. 2015). The Schmidt Hammer operates by measuring the rebound of a spring-driven mass upon impacting a concrete surface, with the rebound value being correlated to compressive strength. Numerous studies have emphasised the importance of correlating Schmidt Hammer results with standard compression tests to improve reliability (Abrams 1927; Malhotra and Carino 2004). However, various factors, including surface roughness, moisture content, concrete age, and material composition, can influence rebound readings and introduce variability (İlhan 2000; Kim et al. 2009;

**CONTACT** A. Yaghoubzadehfard a.yaghoubzadehfard@unimelb.edu.au Department of Infrastructure Engineering, The University of Melbourne, Parkville, VIC 3010, Australia

Malhotra and Carino 2004). Accordingly, calibration and careful interpretation are essential to obtain meaningful data, especially when applied to existing structures with unknown mix designs or exposure histories (Breysse 2012; Brozovsky and Zach 2011). However, in general, it can detect concrete strength in RC structures.

Furthermore, the reinforcement information needed to assess the condition of overall concrete structures can be acquired by using a type of NDT called Profometer. Profometer is a widely used device in the field of civil engineering and construction for non-destructive testing of reinforced concrete structures. It offers reliable methods to assist in assessing the quality and durability of concrete structures. The Profometer works based on the electromagnetic induction principle. When the device is placed on the surface of a concrete structure, it sends out electromagnetic signals which interact with the steel reinforcement inside the concrete. By analysing the reflected signals, the Profometer can accurately determine the location, depth, and diameter of the reinforcement bars, as well as the thickness of the concrete cover (Rogov, Nikolenko, and Sazonova 2021; Tešić, 2021). Some studies have demonstrated the effectiveness and accuracy of the Profometer in various applications. For instance, a study conducted by Rogov et al. (Rogov, Nikolenko, and Sazonova 2021) used the Profometer-5S device to assess the technical condition of reinforced concrete supports of technological overpasses. The results showed that the device could accurately determine the layout of the working reinforcement and the thickness of the concrete cover, which helped in the verification calculations of the structures. Luco (2005) used three equipment, including Profometer to test the cover depth of on-site buildings in Spain and found that all three equipment show the same good performance in shallow covers, and profometer has better performance than the other two for deep covers (Luco 2005).

The objective of this work is to demonstrate an effective framework for assessing ageing RC buildings with limited documentation. By combining NDT results with FEM, the proposed approach addresses knowledge gaps, reduces uncertainty, and supports evidence-based decision-making for repair, retrofitting, or continued service. The methodology is intended to inform future assessment practices for similar structures, particularly in public infrastructure and heritage preservation contexts.

## 2. Methodologies

A flowchart illustrating the overall methodology adopted in this study is presented in Figure 1. The process began with the collection and examination of the available project documentation, which was limited to architectural drawings and a partial technical design file. Due to the absence of complete structural and reinforcement drawings, several assumptions regarding material properties, reinforcement layout, and structural system behaviour were necessary to initiate the modelling process. An initial FEM was developed in ETABS based on these assumptions and geometric data extracted from the architectural plans. To validate and refine the model, a series of non-destructive tests were conducted, including Schmidt Hammer testing to estimate in-situ concrete compressive strength and Profometer scans to determine reinforcement depth, spacing, and arrangement. The experimental data were then integrated into the model to calibrate material parameters and improve the representation of the actual as-built conditions. The updated model was subsequently used for structural assessment and performance evaluation. This integrated methodology enabled reliable structural diagnosis in the absence of complete documentation and demonstrates a practical approach to assessing ageing RC buildings with limited design records.

### 2.1. Case study description

The John Medley Building, located at the University of Melbourne's Parkville Campus, was constructed between

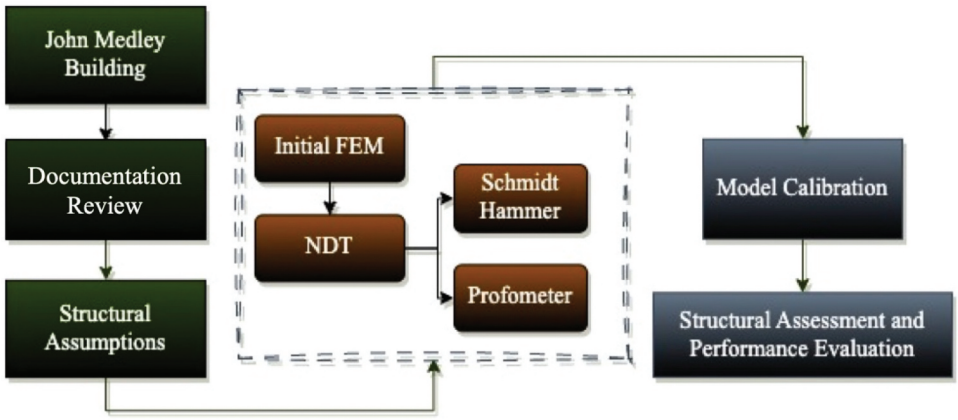


**Figure 1.** Flowchart of the study.

1969 and 1971 to meet the expanding spatial needs of the university's academic departments. The structure comprises two eight-storey RC towers, the East and West Towers, linked by a three-storey bridging section starting from the third floor (see Figure 2).

The primary structural system of the building consists of precast concrete floor slabs supported by reinforced concrete core walls and exterior load-bearing walls. These core walls, located centrally within each tower, provide lateral stability and accommodate vertical circulation and services. The exterior walls, constructed with a combination of reinforced concrete and brickwork, serve both as architectural façades and as part of the gravity load-resisting system.

The bridging section is constructed from exposed aggregate concrete and is integrated into the structural system through cantilevering and transfer elements at the fourth level. Regular column spacing and projected eaves are also notable features that support the multi-level layout and reflect the construction techniques of the late 1960s.

Designed for institutional use, the structure has remained functional for over five decades. However, it is scheduled for demolition by 2040, alongside several other university buildings, as part of a broader campus redevelopment strategy aimed at enhancing open space and upgrading to modern structural performance and sustainability standards.

### 2.2. Documentation review and structural assumptions

A critical challenge encountered in this study was the limited availability of original construction documentation for the RC building under investigation. The only accessible resources were a set of architectural drawings, consisting primarily of floor plans, elevations, and sections, and a single technical document detailing the design of a few individual structural members, such as selected columns and slabs (see Figures 3–5). These documents did not include full structural drawings, reinforcement detailing, or specifications related to material properties, construction methods, or load design criteria. In particular, the absence of a complete structural design package meant that key assumptions regarding the intended structural system, load paths, and design principles had to be inferred rather than verified. Limited information was available on rebar diameters, reinforcement layouts, concrete mix proportions, structural load combinations, or the rationale behind member sizing. Furthermore, the architectural drawings themselves exhibited inconsistencies in scale and notation, which required careful interpretation due to outdated drafting conventions. The summary of the available information is presented in Table 1.

### 2.3. Finite element modelling

A comprehensive finite element model of the case study building was developed using ETABS (Computers and Structures, Inc 2018) to investigate its structural response under service and extreme loading conditions. The structure is an eight-storey RC building, comprising two main blocks, designated as the East and West wings, connected by a three-storey link bridge. The modelling approach aimed to represent the actual geometry, material behaviour, and


Figure 2. John Medley building (a) north elevation, (b) linkage bridge, (c) south elevation, and (d) west elevation.

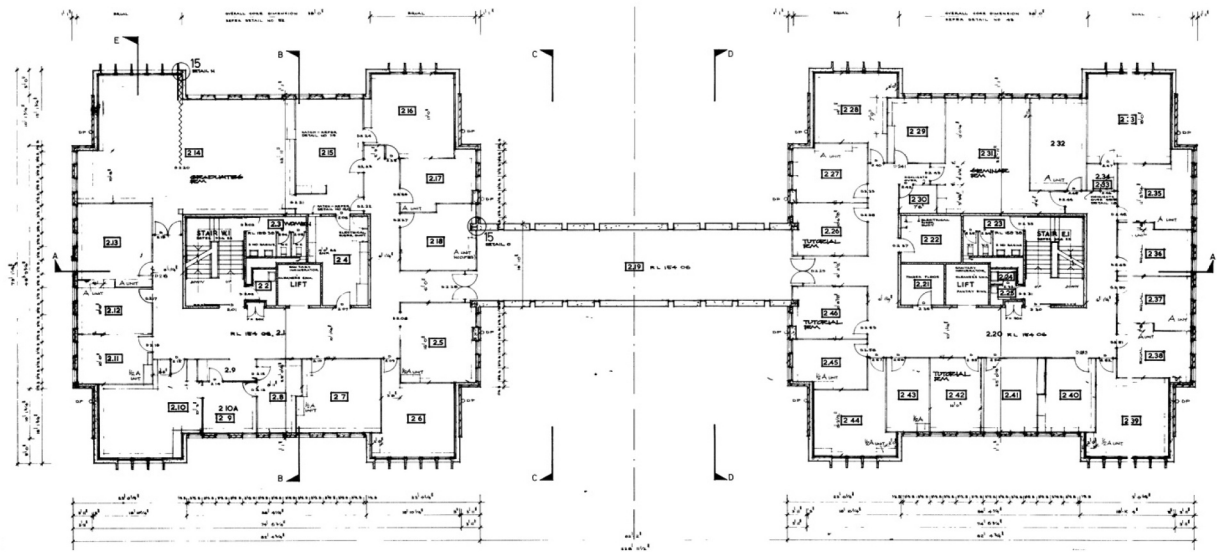

**Figure 3.** Available second floor architectural plan.

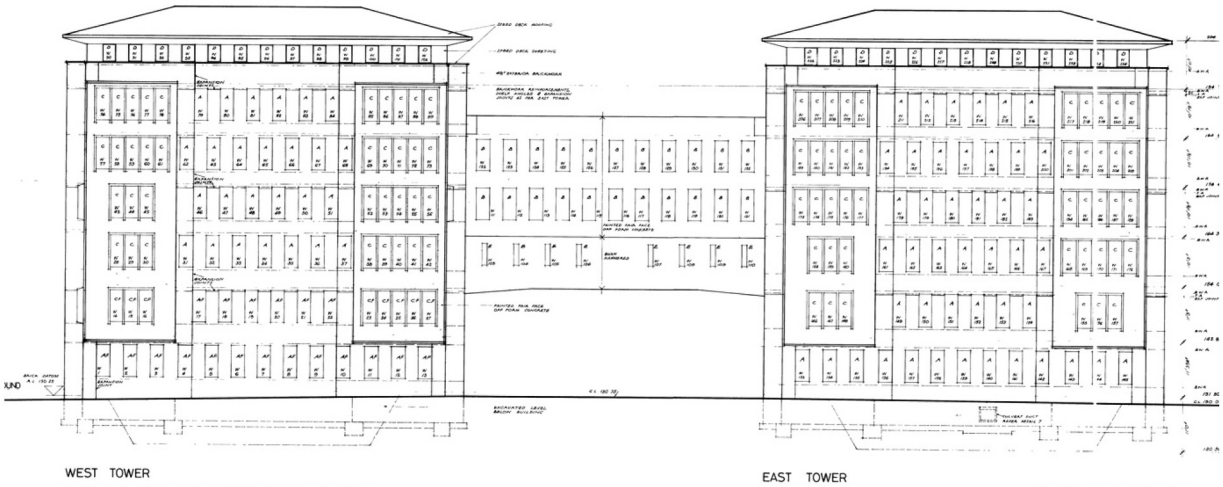


**Figure 4.** Front elevation of the building – west and east towers.

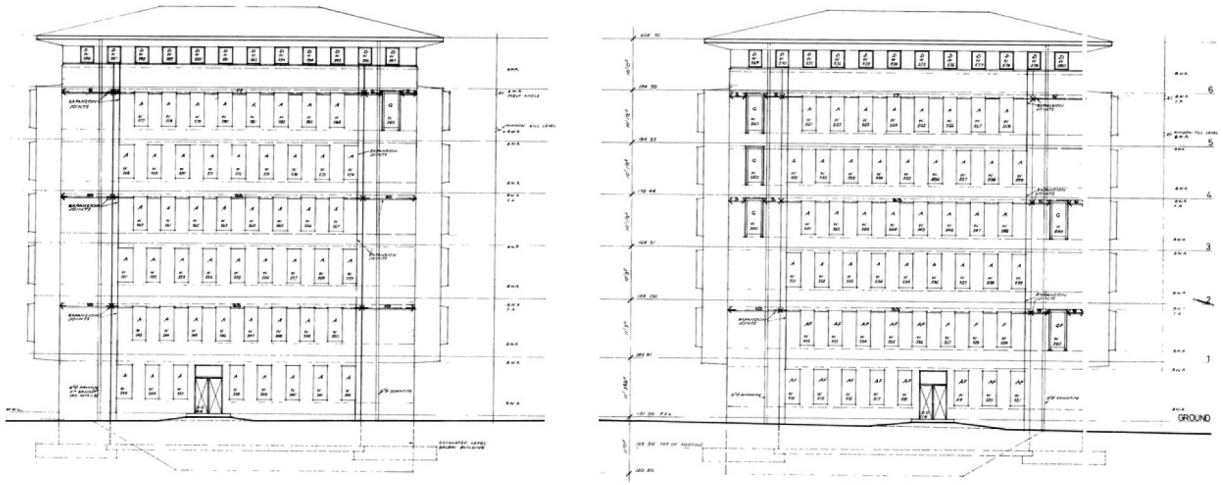


**Figure 5.** Front elevation of the building – south and north towers.

**Table 1.** Summary of available structural documentation.

| Information type | Available | Source | Missing/Assumed |
|---|---|---|---|
| General building geometry | ✓ | Architectural drawings | Used directly (plans, elevations, sections) |
| Floor plans | ✓ | Architectural drawings | Used directly, with some dimensional interpolation where unclear |
| Elevations and sections | ✓ | Architectural drawings | Used directly, minor inconsistencies interpreted based on visual alignment and floors similarity |
| Slab thickness | ✓ | Technical document | 25 cm |
| Structural framing system | ✗ | Architectural drawings | Initially assumed as column-frame; updated to wall system based on visual inspection and NDT |
| Reinforcement layout | ✗ | – | Assumed standard bar arrangements; refined using profometer scans |
| Rebar diameters and spacing | ✓ *(Partial)* | Technical document | Obtained from documents then confirmed via Profometer |
| Concrete strength | ✓ | Technical document | $f_c^{'} = 28MPa$ |
| Concrete mix design | ✗ | – | Not available, assumed standard mix proportions for the period |
| Load combinations and code basis | ✓ *(Partial)* | Technical document | Loading plan partially available |
| Foundation type | ✗ | – | Assumed as raft foundations based on typical practice; not explicitly modelled |
| Steel strength | ✗ | – | Assumed from typical code values |
| Structural drawings (e.g. beam schedules) | ✗ | – | Inferred from geometry and updated with test results |
| Construction method/sequence | ✗ | – | Unknown; |
| Structural modifications/retrofitting | ✗ | – | Not documented, field inspection used to verify presence or absence of alteration |
| Cover depth | ✗ | – | Assumed from typical code values |
| Floor-to-wall connection | ✓ | Technical document | Fixed to core walls and pinned to external walls |

load-resisting systems of the structure as accurately as possible, given the constraints of limited original documentation.

At the preliminary stage, the structural system of each block was assumed to consist of a central reinforced concrete core wall system for lateral load resistance, with discrete columns supporting flat slab floor systems. These assumptions were made based on the available architectural drawings and typical construction practices of the early 1970s. The interconnecting bridge between the two blocks was modelled as a composite system comprising RC slabs supported by steel I-sections embedded within the concrete. However, further investigation through non-destructive testing and site inspections revealed that the initial assumptions underestimated the contribution of the external envelope. Specifically, it was determined that the building incorporates continuous reinforced concrete walls around the perimeter of both blocks, which act not only as vertical load-bearing elements but also contribute significantly to the lateral stiffness of the structure. Consequently, the model was revised to replace the originally assumed column layout with continuous external wall elements. Openings were accurately placed to reflect actual wall discontinuities and their effect on global stiffness and force distribution.

The flooring system in both blocks is a flat slab configuration, which was modelled using shell elements with defined thicknesses and elastic properties representative of typical reinforced concrete slabs. Rigid diaphragms were assigned at each floor level to simulate in-plane stiffness and ensure appropriate load distribution. Additionally, a full basement level was included in the model, enclosed by reinforced concrete retaining walls on all sides. These basement walls were modelled as thick shell elements, providing lateral resistance to soil pressure and contributing to the overall stiffness of the substructure. Appropriate boundary conditions were assigned to represent foundation restraints and ground interaction.

This iterative modelling process, from initial assumptions to a refined configuration based on experimental validation, highlights the importance of integrating site-specific data into numerical models. The final model reflects the actual behaviour of the as-built structure more accurately and serves as a reliable basis for subsequent structural performance assessment and safety evaluation.

### 2.4. Experimental investigations

As mentioned, given the lack of comprehensive structural records, the development of the initial FEM relied heavily on assumptions. To address this, a suite of NDTs, including the Schmidt Hammer and Profometer, was employed on-site to gather empirical data. These tools facilitated the in-situ estimation of concrete strength, reinforcement cover, bar diameters, and layout patterns, which were subsequently used to calibrate and refine the initial model. The integration of these field measurements with the archival documents was essential for developing a realistic and reliable representation of the structure for further structural assessment.

#### 2.4.1. Schmidt hammer

The Schmidt Hammer is a widely used NDT device designed to assess the surface hardness of concrete, which is indirectly related to its compressive strength. The principle of operation is based on the rebound method: a spring-loaded mass is released against the concrete surface, and the extent of rebound after impact is measured. A harder surface results in a higher rebound value, which correlates with greater compressive strength. Traditional Schmidt Hammers display a dimensionless rebound number, which then requires conversion to strength using empirical curves derived from standard cube or cylinder tests (Elrazek and Shafy Gamal 2021). However, the accuracy of these conversions can be affected by factors such as concrete age, surface moisture, carbonation, and aggregate type (Brozovsky and Zach 2011; Kim et al. 2009; Malhotra and Carino 2004).

In this study, a Silver Schmidt PC Type N digital rebound hammer (Proceq 2017) (see Figure 6) was used to perform the surface hardness tests. Unlike analog models, the Silver Schmidt integrates a high-precision sensor system that automatically calculates and displays the estimated compressive strength in MPa, based on internal calibration curves compliant with (CEN 2019; ASTM International 2018; CEN 2012). The device allows the operator to adjust for parameters such as form factor, carbonation correction, and statistical filtering directly on the instrument interface. It also enables digital data export via Hammerlink software for further processing (Proceq 2017).

Prior to testing, all surfaces were prepared by cleaning and lightly grinding to ensure smoothness and remove any laitance. A total of 20 structural elements across the building, including exterior walls, core walls, and columns, were tested. For each element, at least ten impacts were performed, with each point spaced more than 25 mm apart and away from edges or defects. The device's statistical settings were configured to exclude outliers and compute the mean compressive strength per series. All recorded values were displayed and logged directly in MPa (Proceq 2017).

The test results served both as an initial quality assessment of the in-situ concrete and as input for updating the material parameters in the finite element model, particularly considering the building's uncertain construction history.

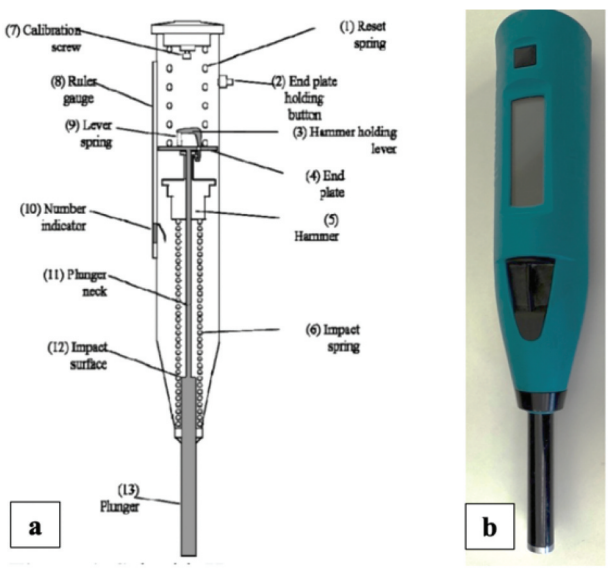


Figure 6. (a) Schematics of Schmidt hammer (Elrazek and Shafy Gamal 2021) (b) a digital Schmidt rebound hammer.

#### 2.4.2. Profometer

In this study, the Profometer 600 (see Figure 7) is used to report the location, cover depth and diameter of reinforcement embedded in the concrete. The Profometer 600, a Switzerland-manufactured instrument, employs electromagnetic pulse induction technology to detect rebars in concrete (Rogov, Nikolenko, and Sazonova 2021). The measurement of the Profometer 600 is unaffected by non-conductive materials but influenced by conductive ones within a 100 mm radius magnetic field. Delivered with components like a touchscreen unit, battery, probe, and


Figure 7. A profometer 600 unit.

software, it features a 7-inch display, 8GB storage, and over 8-hour battery life (Proceq 2014).

The Profometer 600 testing procedure begins with equipment preparation: ensure all components (touchscreen unit, probe, battery, cables) are properly connected and calibrated. Power on the device by pressing the designated button and confirming the battery status (Proceq 2014).

Prior to measurement, settings were configured, including measuring range (Standard, Large, or Auto), rebar diameter, unit (Metric or Imperial), and minimum/maximum cover values. Zeroing should be performed to ensure accuracy, especially if the probe has been idle for over 5 minutes.

There are different testing modes, including locate mode, single-line mode, multi-line mode, and area-scan mode in the Profometer 600 (Proceq 2014). In this study, we use multi-line mode. When we turn to the multi-line mode, the rebar positions can be identified by moving the probe until the centre line of the probe aligns with the embedded rebar, indicated by LED signals. Then, the measurement of the diameter of the rebar can be taken by clicking on the button of measurement on the screen. Then, a constant speed of scanning is maintained to move to the next rebar to take the measurement. The measurements are recorded by saving files with unique names, ensuring each dataset includes cover depth, rebar diameter, and spacing. After measurement, the data can be reviewed via Statistics or Snapshot views to verify accuracy. Finally, the data can be exported using the PM-Link software for further analysis.

## 3. Results and discussion

This section presents the outcomes of the NDT and the updated FEM, followed by a structural reassessment under current Australian standards. The primary goal of this integrated approach was to establish a reliable representation of the as-built condition and to evaluate whether the structure complies with contemporary performance requirements. The Schmidt hammer and Profometer tests were used to characterise material strength and reinforcement details, which informed the calibration of the finite element model. The structural response was then analysed under historical and modern code provisions to assess the adequacy of the building's design. The findings reveal notable discrepancies between the original design assumptions and the demands imposed by current standards, ultimately leading to the conclusion that several key structural components fail to meet the required performance thresholds.

### 3.1. Non-destructive testing results

The results of the digital Schmidt hammer test were critical in reassessing the structural system of the building. As shown in Table 2, external wall elements across both the West and East blocks exhibited consistently high compressive strength values, including areas situated above and below window openings. This uniformity strongly suggests that these walls were designed as continuous load-bearing elements, rather than as non-structural infill or façade components. In contrast to the initial assumption of a beam–column frame system, the data supports a wall-dominant structural configuration, prompting a revision of the FEM to accurately represent the observed in-situ conditions.

The test data also revealed substantial increases in concrete strength compared to the original design value of 28 MPa. In external wall elements, estimated strengths frequently exceeded 56 MPa, an increase of up to 200%. Core walls showed more moderate gains, with values ranging from approximately 38 to 42 MPa, or about 40% above the design value. These strength increases are likely attributable to long-term material behaviour, including continued hydration, internal curing, and surface carbonation, particularly in elements more exposed to ambient conditions. Furthermore, Schmidt hammer measurements are surface-hardness based and may overestimate the true in-situ compressive strength of older concrete, especially where carbonation has densified the cover zone (e.g. external walls). Aydin and Saribiyik (2010)

**Table 2.** Compressive strength of elements obtained from Schmidt hammer test.

| Element ID | Location | Element Type | Average estimated $f_c^{'}$(MPa) |
|---|---|---|---|
| 1 | West block – 1st floor | Core wall | 40 |
| 2 | | External walls | 61 |
| 3 | | Column | 63 |
| 4 | | Slab | 59 |
| 5 | | Stairs | 43 |
| 6 | West block - Roof | External walls | 61 |
| 7 | | Slab | 60 |
| 8 | East block – 1st floor | Core wall | 40 |
| 9 | | External walls | 60 |
| 10 | | Column | 61 |
| 11 | | Slab | 60 |
| 12 | | Stairs | 42 |
| 13 | East block- Roof | External walls | 61 |
| 14 | | Slab | 60 |

recommend applying correction factors of approximately 0.50–0.80 for concrete older than 90 days, while Kazemi, Madandoust, and de Brito (2019) showed that Schmidt hammer results can misestimate compressive strength when used in isolation, with rebound-based estimates being, on average, about 45% higher than reference values. Nonetheless, when interpreted as an index of relative strength, the Schmidt hammer data in this study provide clear and repeatable trends across structural elements, supporting the identification of load-bearing behaviour and informing material property selection within the analytical model, while acknowledging the inherent limitations of the method for absolute strength quantification. Due to the building's ongoing operational use, intrusive core testing was not feasible. Consequently, Schmidt hammer results were interpreted as relative indices of in-situ strength rather than absolute values, and conservative strength values were adopted in the FEM calibration.

Profometer testing was carried out at the same locations assessed by the Schmidt hammer to clarify reinforcement detailing, given the absence of structural drawings. The data helped verify the size, spacing, and layout of reinforcement in key structural elements across both the West and East blocks, as well as the linking bridge. Reinforcement patterns largely aligned with typical construction practices of the 1970s, though minor deviations were observed near intersections and slab edges.

Importantly, the scans confirmed that the external walls, particularly those containing window openings, featured continuous vertical reinforcement extending across storeys. This finding reinforced the earlier conclusion that these façades were designed as integral load-bearing walls, not infill. Concrete cover depth was also recorded, generally ranging from 40 to 75 mm. These measurements contributed to model calibration and informed preliminary assessments of durability.

A 3-metre linear scan was conducted along the longitudinal axis of the central core wall using a Profometer rebar detector in single-line mode. The resulting signal data, as illustrated in Figure 8, provides critical insights into the spacing, bar diameter, and cover depth of the vertical reinforcement. The scan identified a regular pattern of signal peaks corresponding to embedded longitudinal reinforcement bars, with consistent signal amplitudes indicative of relatively uniform bar placement. The spacing between adjacent bars varied slightly across the scan length, with measured centre-to-centre distances ranging approximately from 16 mm to 26 mm, suggesting an average bar spacing of roughly 250 mm. The Profometer software algorithm estimated bar diameters primarily in the range of 16 mm to 26 mm, with most bars detected as 16–20 mm, and isolated peaks indicating larger diameters (up to 26 mm) likely due to overlapping bars or calibration inaccuracies. Using the same procedure, additional Profometer scans were conducted at key structural locations throughout the building, including the mid-height and upper zones of the core wall, selected external wall segments at base and window lintels, and representative slab zones adjacent to the core and at roof level. The reinforcement layout obtained in these regions was generally consistent with the pattern observed in the core wall base, with no indication of seismic-specific detailing features such as confined boundary elements, closely spaced transverse ties, or mechanical anchorage. These findings suggest that the reinforcement system throughout the building reflects conventional gravity-load design practice rather than detailing intended for ductile seismic performance. Table 3 summarises the Profometer test results, highlighting average bar sizes, spacing, and concrete cover values across the major structural elements.

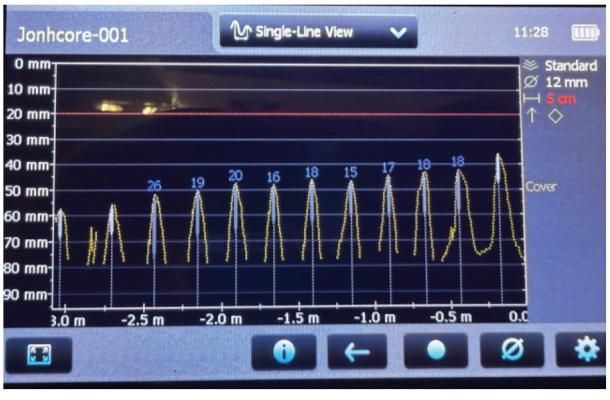


**Figure 8.** Results obtained from Profometer.

Following the non-destructive testing and field investigations, the FEM was updated to reflect more realistic structural assumptions based on verified in-situ conditions. This led to significant modifications to the initial model, which had been developed solely from architectural drawings and a partial technical document (Figure 9). The revised model incorporated corrected structural system definitions, including the replacement of assumed column layouts with continuous external walls, updated material properties, and verified reinforcement details. The updated FEM is presented in Figure 10 and provides a more reliable

**Table 3.** Profometer test summary table.

| Element | Rebar size (mm) | Spacing (mm) | Average cover (mm) |
|---|---|---|---|
| Core wall | 19 | 250 | 45 |
| External walls North and South | 19 | 250 | 55 |
| External walls East and West | 19 | 200 | 55 |
| Slab | 16 | 200 | 40 |

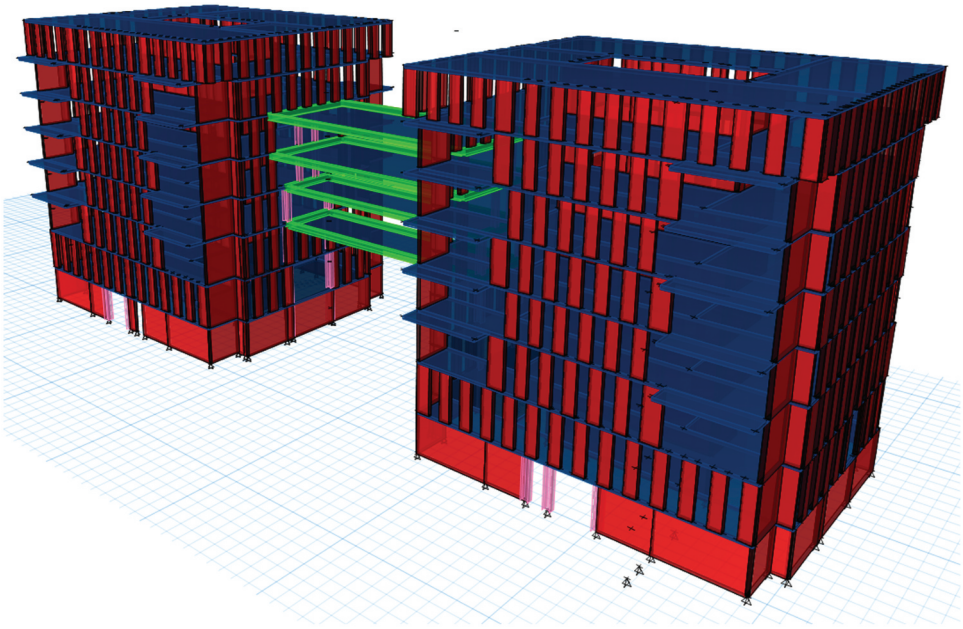

**Figure 9.** Initial FEM of the building.

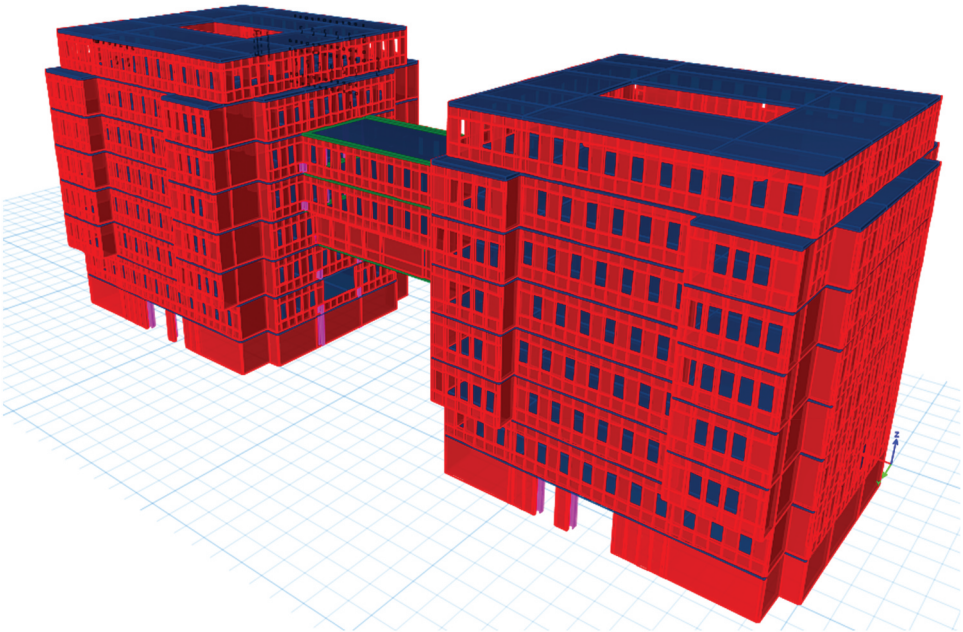

**Figure 10.** Updated FEM of the building.

representation of the as-built structure. This process highlights the critical role of documentation, both in terms of its availability and ongoing management. Maintaining comprehensive and accurate records throughout a structure's life cycle is essential, not only for future assessment and retrofitting but also for ensuring safety and cost-effective decision-making over time.

To evaluate the ductility characteristics and reinforcement detailing of the existing building, a comprehensive non-destructive investigation was undertaken using a Profometer. The scan was performed at strategic vertical levels and structural elements, including: (i) the base, mid-height, and top of the core wall; (ii) base regions and lintel zones of external walls; (iii) slabs adjacent to the core wall; and (iv) the roof slab. The objective was to characterise reinforcement spacing, bar diameters, and cover depth, which are critical parameters in assessing ductility and compliance with modern seismic detailing requirements.

The collected data revealed that the reinforcement configurations in all scanned regions lack the features typically associated with ductile behaviour. In particular, the core wall exhibited relatively wide bar spacing, uniform bar diameters without evidence of confining

reinforcement (e.g. closely spaced ties or stirrups), and inadequate cover depth in some locations. Similar deficiencies were observed in the external walls and slabs, including minimal reinforcement concentration near critical regions such as openings and slab–wall interfaces. These findings suggest an absence of ductility-enhancing detailing, such as confined boundary zones in walls, adequate anchorage lengths, or transverse reinforcement designed to resist cyclic loading.

Given that ductile design provisions only became mandatory in Australian Standards following the introduction of AS 3600–1988 and later enhancements in AS 1170.4, the observed reinforcement layout is consistent with pre-ductility-era construction. Therefore, the structure is likely to exhibit limited energy dissipation capacity and poor post-yield deformation performance during seismic events. This raises concern for structural resilience and necessitates further evaluation or retrofit considerations in accordance with current performance-based seismic assessment frameworks.

To quantify the implications of the observed reinforcement detailing under current design provisions, a comparison between provided and required reinforcement areas was carried out in accordance with AS 3600, as summarised in Table 4.

## 3.2. Structural reassessment under modern code: failure causes and code comparison

The evolution of Australian Standards for structural loading has introduced substantial changes in how buildings are assessed. The building under investigation, constructed in the early 1970s, likely adhered to provisions from SAA Int 350 (SAA Int 350 1952). In contrast, modern evaluations are governed by AS/NZS 1170 series (AS 1170.2 2021; AS 1170.4 2024; AS/NZS 1170.1 2002, which adopt a limit state design (LSD) framework with detailed probabilistic load combinations and reliability targets.

### 3.2.1. Dead and live (imposed) loads

SAA Int 350 (*Standards Association of Australia, 1952*) presented dead and live loads as simplified prescriptive values, expressed in imperial units and largely based on occupancy type and engineering judgement. For commercial buildings, live loads were assigned using occupancy tables, and dead loads were treated as uniform values with minimal adjustment for material variability. There was limited guidance on load combinations or variability due to functional use. In comparison, AS/NZS 1170.1 (Standards Australia/Standards New Zealand 2002) introduces the terminology of permanent actions (dead loads) and imposed actions (live loads), reflecting ISO alignment. It provides comprehensive load values based on building usage, floor area, and load duration, with probabilistic load factors applied for ultimate and serviceability limit states (Pham 2007). Additionally, the modern standard explicitly defines load combinations (e.g. 1.2 G + 1.5Q) and accounts for reduced imposed loads in multi-storey buildings, acknowledging the improbability of simultaneous full loading across all floors.

### 3.2.2. Wind loads

A major shift is observed in the treatment of wind loads. SAA Int 350 (Standards Association of Australia, 1952) used a uniform average wind velocity of 75 mph (33 m/s) with basic reduction factors for multiple-bay buildings (e.g. 0% windward, 50% first leeward), based on empirical simplifications (Mackenzie, Rowland, and Johnsson 2017). Internal pressure effects were considered rudimentarily, and terrain or topography factors were largely absent. In contrast, AS 1170.2 (AS 1170.2 2021) provides a sophisticated framework for wind actions, incorporating gust wind speeds, terrain categories, topographic multipliers, shielding effects, and directional multipliers. The shift to gust-based design, inspired by the work of John Holmes and others, significantly increased calculated uplift and suction pressures, particularly for external walls and roofing systems. This has profound implications for buildings retrofitted or re-analysed under the current code, often leading to requirements for structural strengthening (Mackenzie, Rowland, and Johnsson 2017).

### 3.2.3. Earthquake loads

Earthquake loading under SAA Int 350 (Standards Association of Australia 1952) was absent. The

**Table 4.** Comparison of provided and required reinforcement areas for key structural elements under AS 3600 assessment.

| Elements | | | Provided reinforcement ($mm^2$) | Required reinforcement ($mm^2$) |
|---|---|---|---|---|
| External walls | Piers | | 7371.74 | 8836 |
| East and West side | Lintels | | 490.87 | 738 |
| External walls | Piers | | 14743.49 | 11712 |
| North and South side | Lintels | | 490.87 | 738 |
| Core walls | – | | 99802.11 | 119543 |
| Slab roof | Top | x-dir. | 2491 | 2100.6 |
| | Bottom | x-dir. | 2491 | 2100.6 |
| | Top | y-dir. | 1721 | 1570.75 |
| | Bottom | y-dir. | 1721 | 1570.75 |

development of a dedicated standard, AS 2121(AS 2121 1979), marked the beginning of codified seismic design in Australia, but it remained separate from other actions. Modern practice under AS 1170.4 (AS 1170.4, 2007) integrates seismic actions into the LSD framework, applying zonal seismic hazard values, importance levels, ductility factors, and site classification. This allows for a quantifiable and risk-informed approach to seismic design. As outlined by (Pham 2007), the integration of seismic loading into the AS 1170 series allowed Australia to consolidate design practices under a unified structural action code and improve structural safety expectations under rare seismic events.

In reviewing the structural loads applicable to the building's design and reassessment, it becomes evident that substantial differences exist between the historical code (SAA Int 350) and the current AS 1170 standards. These differences are not limited to the magnitude of the loads but also extend to how variability, safety margins, and environmental influences are accounted for. The progression towards more performance-based and reliability-focused design frameworks in AS 1170 results in more comprehensive, and often more conservative, load estimations, particularly for wind and seismic actions. Such changes have direct implications when re-evaluating older structures originally designed under earlier codes, as they may reveal previously unaccounted vulnerabilities or the need for structural retrofitting. A summary of the key differences is presented in Table 5, providing a concise comparison across load types for reference in both modelling and compliance considerations.

In addition to changes in loading assumptions, a significant evolution has occurred in the design methodology and capacity calculation for reinforced concrete structures. The original design of the case study building likely followed AS CA2–(1963) (AS CA2 1963), which was grounded in the Working Stress Design (WSD) approach. This method assumed linear elastic behaviour for both concrete and steel, with service loads directly compared to allowable stresses using conservative safety margins. Material properties were less diverse, with concrete strengths typically in the range of 20–25 MPa and mild steel reinforcement limited to approximately 230 MPa yield strength. Detailing provisions were also minimal, and vital concepts such as ductility, redistribution limits, or crack width control were either absent or only qualitatively addressed.

In contrast, the current design practice under AS 3600–(2018) (AS 3600 2018) adopts the Limit State Design (LSD) philosophy. This approach incorporates strength reduction factors probabilistic load combinations, and material-specific ductility considerations to ensure safety under both ultimate and serviceability conditions. Concrete grades have increased significantly, commonly ranging from 32 MPa to 50 MPa or higher, and high-strength reinforcement with a 500 MPa yield stress is now standard. The modern code also includes detailed rules on reinforcement spacing, anchorage, cover, and moment redistribution (up to 30%), which allows for more refined and reliable modelling of actual structural performance.

Table 6 summarises the principal differences between these two standards across key design parameters. This comparison underscores the broader shift from prescriptive, stress-based approaches to performance-driven design with more realistic treatment of structural behaviour and uncertainty.

To evaluate how shifts in structural standards influence performance assessment, the updated finite element model, calibrated using field data, was analysed

**Table 5.** Comparing SAA int 350 and AS 1170.

| Load type | SAA Int 350 | AS 1170 series |
|---|---|---|
| Dead loads | Fixed prescriptive values in imperial units | Probabilistic "permanent actions" with load factors |
| Live loads | Occupancy-based, no duration or frequency adjustment | Varying "imposed actions" with reductions for floor usage |
| Wind loads | Mean wind speed (75 mph), simple bay reduction | Gust wind speed, terrain/topography effects, direction factors |
| Earthquake loads | Not codified | Fully integrated LSD framework with zonal hazard mapping |

**Table 6.** Comparison of AS CA2–(1963) and AS 3600–(2018) design parameters.

| Design Parameter | AS CA2–(1963) | AS 3600–(2018) |
|---|---|---|
| Design Philosophy | Working Stress Design (WSD) | Limit State Design (LSD) |
| Concrete Design Method | Linear elastic; stress-based | Ultimate strength; strain-based |
| Steel Design Method | Elastic theory, mild steel assumed | Strength design with ductility limits |
| Concrete Strength Grades | Typically 20–25 MPa | Commonly 32–50 MPa or higher |
| Reinforcement Yield Strength | 230 MPa (mild steel) | 500 MPa (typical high strength) |
| Strength Reduction Factors | Not explicitly used | Typically, 0.6 for bending; 0.8 for shear |
| Maximum Compression Strain | 0.003 | 0.003 (explicitly defined) |
| Serviceability Criteria | Based on deflection/span rules | Detailed SLS checks including crack width |
| Reinforcement Placement Limits | Basic guidance, limited detailing | Detailed rules for spacing, anchorage, cover |
| Moment Redistribution | Not well defined | Allowed up to 30% under conditions |

under two distinct code regimes. The first scenario reflects the design philosophy in place at the time of construction, using load assumptions from SAA Int 350 (1952) and material design provisions from AS CA2–(1963), which governed the design of reinforced concrete structures in that era. The second scenario applies the modern loading framework defined in the AS/NZS 1170 series, in combination with the current AS 3600–(2018) standard for concrete structures.

While both models share the same geometry and in-situ material properties, the structural responses and compliance margins diverge significantly due to differences in load magnitudes, combination rules, and capacity calculation methods. Under historical codes, design stresses were assessed using the working stress method, with relatively lower safety factors and simpler assumptions about material behaviour. In contrast, AS 3600 adopts a limit state design (LSD) approach with detailed guidance on strength reduction factors, ductility considerations, and redistribution limits.

The analyses revealed that, when assessed using AS 3600 and current load standards, several elements, particularly the external walls and the link bridge components, experience higher demand-to-capacity ratios, often approaching or marginally exceeding allowable thresholds. Lateral displacements, base shear, and inter-storey drifts were consistently higher under AS 1170 seismic actions, due to more rigorous treatment of dynamic and environmental factors. Furthermore, the moment and shear capacities of key RC members calculated under AS 3600 tended to be more conservative, especially for lightly reinforced sections, compared to historical assumptions. These findings underscore the potential vulnerability of older structures when re-evaluated against current performance expectations and highlight the importance of integrating both loading and capacity code updates in structural re-assessment.

## 4. Conclusion

This study presents a practical methodology for the structural evaluation of a reinforced concrete building constructed in 1971 with limited available documentation. Through the integration of numerical modelling and targeted non-destructive testing, a reliable structural representation was achieved despite the absence of detailed construction records. The initial finite element model, based solely on architectural drawings and typical assumptions, was iteratively updated using in situ data obtained from Schmidt hammer and Profometer tests.

Compressive strength results from the Schmidt hammer revealed values significantly higher than the original design specification, particularly in external wall elements, where strengths frequently exceeded 55 MPa. These elevated values, attributed to long-term hydration and environmental exposure, supported the reclassification of the external envelope as a primary load-bearing system. Profometer scans confirmed the presence of continuous vertical reinforcement and identified bar sizes and spacing consistent with historical norms. Collectively, these findings prompted a fundamental shift in the structural interpretation from a column slab frame to a wall dominated system.

Despite favourable material performance, the reinforcement layout lacked critical features associated with ductile response. Wide spacing, uniform bar diameters, and the absence of confinement detailing were evident across core walls, slabs, and façades. This is consistent with the pre-ductility design provisions of the era. When the updated model was assessed under the AS 1170 and AS 3600 standards, multiple components, particularly in the external walls and bridge connections, failed to satisfy current structural performance requirements. Demand-to-capacity ratios exceeded acceptable thresholds in key regions, highlighting deficiencies in lateral stiffness and energy dissipation.

These results demonstrate that reliance on original design documentation alone is insufficient for reliable structural evaluation of older buildings. The integration of field measurements into a calibrated numerical model offers a pathway to more accurate assessment, supports informed engineering judgement, and enables risk-based decision making for retrofit, continued service, or demolition.

To further improve the accuracy of the assessment and address residual uncertainties, future studies may incorporate more advanced non-destructive and remote sensing techniques. For instance, ground penetrating radar can be employed to investigate subsurface conditions such as moisture ingress and reinforcement corrosion, which are critical to long-term durability but are not fully captured through surface-based testing. The use of IBIS-FS interferometric radar also presents a promising direction for operational modal analysis under ambient conditions. By capturing real-time displacement responses, the natural frequencies and mode shapes of the structure can be identified and compared against numerical predictions. This enables model updating and enhances confidence in dynamic behaviour predictions, particularly under wind and seismic loading.

However, persistent uncertainties related to as-built construction, including connection detailing, material variability, and construction quality, continue to complicate model calibration. A Bayesian updating framework can be applied to integrate field data with assumed parameters, enabling

probabilistic calibration and improved prediction fidelity. This approach is especially valuable when complete records are unavailable. Furthermore, changes in reinforcement detailing practice over recent decades should be acknowledged. Earlier standards, such as AS CA2 provided limited guidance on anchorage, splicing, and seismic resistance. In contrast, AS 3600 introduces rigorous criteria for ductility, confinement, and serviceability. Detailed investigation of reinforcement layouts through high-resolution scanning or targeted core extraction may therefore support improved model refinement and structural reliability assessment in future applications.

## Acknowledgments

This research was supported by the ABP-FEIT Research Collaboration Development Grant 2024, awarded by the University of Melbourne. The authors gratefully acknowledge this support, which made this study possible.

## Author contributions

CRediT: **A. Yaghoubzadehfard:** Conceptualization, Data curation, Formal analysis, Investigation, Methodology, Software, Validation, Visualization, Writing – original draft; **Z. Zhou:** Investigation, Writing – original draft; **N. Herath:** Funding acquisition, Project administration, Supervision, Writing – review & editing; **M. Sofi:** Methodology, Resources, Writing – review & editing; **E. Lumantarna:** Validation, Writing – review & editing; **P. Mendis:** Project administration, Supervision, Writing – review & editing; **P. Vaz-Serra:** Project administration, Supervision; **K. Day:** Writing – review & editing; **X. Ma:** Writing – review & editing.

## Disclosure statement

No potential conflict of interest was reported by the author(s).

## ORCID

A. Yaghoubzadehfard http://orcid.org/0000-0002-7303-9825

## References

Abrams, D. A. 1927. "Water-Cement Ratio as a Basis of Concrete Quality." *Journal Proceedings* 23 (2): 452–457.

Alyamac, K. E., E. Ghafari, and R. Ince. 2017. "Development of Eco-Efficient Self-Compacting Concrete with Waste Marble Powder Using the Response Surface Method." *Journal of Cleaner Production* 144:192–202. https://doi.org/10.1016/j.jclepro.2016.12.156.

ASTM International. 2018. *Standard Test Method for Rebound Number of Hardened Concrete (ASTM C805)*. PA, USA: ASTM International.

Aydin, F., and M. Saribiyik. 2010. "Correlation Between Schmidt Hammer and Destructive Compression Testing for Concretes in Existing Buildings." *Scientific Research and Essays* 5 (13): 1644–1648.

Breysse, D. 2012. "Nondestructive Evaluation of Concrete Strength: An Historical Review and a New Perspective by Combining NDT Methods." *Construction and Building Materials* 33:139–163. https://doi.org/10.1016/j.conbuildmat.2011.12.103.

Brozovsky, J., and J. Zach. 2011. "Influence of Surface Preparation Method on the Concrete Rebound Number Obtained from Impact Hammer Test." *Pan American Conference for NDT* 16 (12). https://www.ndt.net/?id=11196.

CEN. 2012. *Testing Concrete – Part 2: Non-Destructive Testing – Determination of Rebound Number*. European Committee for Standardization.

CEN. 2019. *Assessment of In-Situ Compressive Strength in Structures and Precast Concrete Components*. European Committee for Standardization.

Computers and Structures, Inc. 2018. "*ETABS 2018: Integrated software for structural analysis and design*."

Elrazek, M. A., and Y. A. Shafy Gamal. 2021. "The Reliable Concrete Compression Strength Assessment by Schmidt Hammer for Different Concrete Grades." *IOP Conference Series: Materials Science and Engineering* 1171 (1): 012004. https://doi.org/10.1088/1757-899X/1171/1/012004.

İlhan, İ. 2000. "What Does the Schmidt Hammer Do?" *TMH - Turkish Engineering News* 410:26–28.

Kazemi, M., R. Madandoust, and J. de Brito. 2019. "Compressive Strength Assessment of Recycled Aggregate Concrete Using Schmidt Rebound Hammer and Core Testing." *Construction and Building Materials* 224:630–638. https://doi.org/10.1016/j.conbuildmat.2019.07.110.

Kim, J. K., C. Y. Kim, S. T. Yi, and Y. Lee. 2009. "Effect of Carbonation on the Rebound Number and Compressive Strength of Concrete." *Cement and Concrete Composites* 31 (2): 139–144. https://doi.org/10.1016/j.cemconcomp.2008.10.001.

Luco, L. F. 2005. "Comparative Test, Part II: Comparative Test of "Covermeters"." *Materials and Structures* 38 (10): 907–911. https://doi.org/10.1007/BF02482257.

Mackenzie, N., G. Rowland, and S. Johnsson. 2017. "Wind Engineering Applied to Heritage Structures." Proceedings of the 9th Asia-Pacific Conference on Wind Engineering (APCWE-IX), University of Auckland, Auckland, New Zealand. Figshare.

Malhotra, V. M., and N. J. Carino. 2004. *Handbook on Nondestructive Testing of Concrete*. CRC Press.

Pham, L. 2007. "Actions on Structures: Regulations and Standards." *Electronic Journal of Structural Engineering (EJSE), Special Issue: Loading on Structures*: 1–8. https://ejse.org/2007/Actions-on-Structures-Regulations-and-Standards.pdf.

Proceq, S. A. 2014. Profometer PM-600/PM-630: Operating Instructions.

Proceq, S. A. 2017. Silverschmidt & Hammerlink: Operating Instructions. https://www.proceq.com.

Rogov, N. Y., S. D. Nikolenko, and S. A. Sazonova. 2021. "Modeling the Process of Inspection of Reinforced Concrete Supports of Technological Overpasses." *Modeling of Systems and Processes* 14 (1): 5. https://doi.org/10.12737/2219-0767-2021-14-1-68-73.

Standards Association of Australia. 1952. *SAA INT 350: Minimum Design Loads on Buildings*. Standards Australia.

Standards Association of Australia. 1963. *AS CA2: SAA Concrete Structures Code*. Standards Australia.
Standards Association of Australia. 1979. *AS 2121: The Design of Earthquake-Resistant Buildings*. Standards Australia.
Standards Australia. 2018. AS 3600: Concrete Structures.
Standards Australia. 2021. "AS 1170.2: Structural Design Actions – Part 2: Wind Actions."
Standards Australia. 2024. AS 1170.4: Structural Design Actions – Part 4: Earthquake Actions in Australia.
Standards Australia/Standards New Zealand. 2002. AS/NZS 1170.1: Structural Design Actions – Part 1: Permanent, Imposed and Other Actions.
Tešić, K. 2021. "Comparison of Cover Meter and Ground Penetrating Radar Performance in Structural Health Assessment: Case Studies." *Građevinar* 73 (11): 1131–1144. https://doi.org/10.14256/JCE.3323.2021.
Yılmaz, N., and Ö. Avşar. 2013. "Structural Damages of the May 19, 2011, Kütahya-Simav Earthquake in Turkey." *Natural Hazards* 69 (1): 981–1001. https://doi.org/10.1007/s11069-013-0747-2.
Yon, B., E. Sayin, Y. Calayir, Z. C. Ulucan, M. Karatas, H. Sahin, A. T. Bildik, and A. T. Bildik. 2015. "Lessons Learned from Recent Destructive Van, Turkey Earthquakes." *Earthquakes and Structures* 9 (2): 431–453. https://doi.org/10.12989/eas.2015.9.2.431.